

## Settlement of River Dykes and Their Adjacent Residences on Soft Clay Deposits After the Tohoku-Pacific Ocean Earthquake in 2011

K. Yasuhara<sup>1</sup>, S. S. Yang<sup>2</sup>, I. Horikawa<sup>2</sup> and H. Yamane<sup>2</sup>

<sup>1</sup> Institute for Global Change Adaptation Science, Ibaraki University, 2-1-1 Bunkyo, Mito, Ibaraki, 310-8512, Japan

<sup>2</sup> Construction Technology Research Institute, 1-14-6, Kamikizaki, Urawa-ku, Saitama-shi, Saitama, 330-0071, Japan

E-mail: kazuya.yasuhara.0927@vc.ibaraki.ac.jp

**ABSTRACT:** Among the extensive infrastructure collapses which resulted from the cataclysmic earthquake that struck off the eastern coast of Japan on March 11, 2011, long-term settlement and deformation of clay deposits during the earthquakes has sometimes been overlooked. This paper describes a case history of post-earthquake settlement of clay deposits underlying river dykes and their adjacent residences. Particularly, an attempt is made to assess reactive countermeasures designed to mitigate damage from such settlement and deformation.

**KEYWORDS:** Land subsidence, Earthquake, Clay deposit, Countermeasure

### 1. INTRODUCTION

Land subsidence and ground sinking are as remarkable and as extremely destructive phenomena as the gigantic tsunami that struck Tohoku and Kanto in Japan after the 2011 Off the Pacific Coast of Tohoku Earthquake (hereinafter the “Tohoku Earthquake”). Moreover, the mechanisms of both events are complex because several tectonic, geologic, and geotechnical factors induced land subsidence and ground sinking, exerting overlapping influences that persist even now, six years after the earthquake.

Roughly speaking, this land subsidence and ground sinking are classifiable into three categories: (i) land sinking along coastal areas because of tectonic movements (Imakiire and Koarai, 2012, Yasuhara and Kazama, 2015), (ii) settlement of sandy deposits and subsequent liquefaction, and (iii) long-term post-earthquake settlement in soft clay caused by the dissipation of excess pore pressure. Land subsidence of the latter two categories (ii) and (iii) occurs in inland areas, strongly influencing local residents. A difference is apparent between the settlement mechanisms of both types in the settlement of category (ii), which is related to saturated sandy deposits, whereas the settlement in category (iii) is associated with saturated clayey deposits. Based on differences among the causes and mechanisms related to the land subsidence of three kinds described above, suitable countermeasures against subsidence must be taken, corresponding to their different characteristics.

This paper presents a case study of post-earthquake settlement and deformation of clay deposits underlying the river dykes and their adjacent residences in Ibaraki during and after the Tohoku earthquake in 2011, including the effects of countermeasures which were undertaken immediately after the earthquake.

### 2. RIVER DYKE AND RESIDENCE DAMAGE

#### 2.1 Acceleration waveform

The waveform measured 15 km distant from the river dyke exhibited 6-weak seismic intensity (on the Japanese scale) during the Tohoku Off-Pacific Earthquake in 2011, as shown in Figure 1.

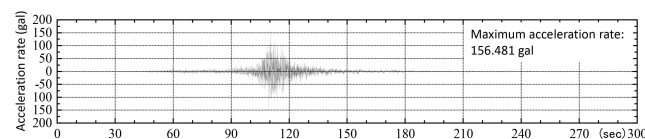


Figure 1 Acceleration waveform measured near the river dyke

#### 2.2 Damage features of the river dykes and their vicinity

Some features of damage to the objective river dyke in Ibaraki Prefecture after the Tohoku earthquake is presented in Photo 1.



(a) River dyke failure



(b) Damage to the sluice pipe



(c) Damage to the residence outer wall

Photo 1 Damage features after the earthquake

Damage to the river dyke and the sluice pipe was remediated soon after the earthquake. However, damage to residences including

cracks in the exterior walls was recovered completely or was left for discussion among residents and the government because it was not certain which factors were responsible for increasing damage to residences, although settlement and inclination had been observed since the start of river dyke construction, as explained later in this paper. In any case, long-term settlement and deformation are expected to result from existence of the thick clay layer underlying the sand layer, having the soil profile shown in Figure 2.

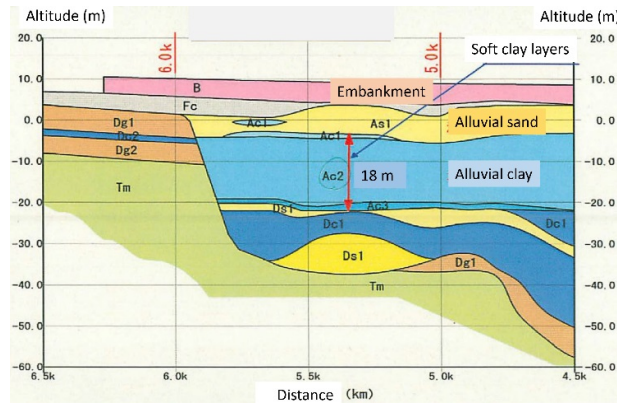


Figure 2 Geological profile of the objective site.

### 3. EARTHQUAKE-INDUCED SETTLEMENT OF CLAY DEPOSITS

#### 3.1 Earthquake-induced settlement

Liquefaction-induced settlement of sandy soil deposits ceases quickly, but cohesive soil deposit settlement takes a long time to end because of the low hydraulic conductivity of cohesive soils and the slow dissipation of excessively high pore pressure generated during earthquakes (Yasuura et al., 2001; Yasuura and Matsuda, 2002; Matsuda et al., 2014). It continues from the instant of settlement immediately after the earthquake. Therefore, earthquake-induced residual settlement of cohesive soil deposits includes instant settlement (non-time dependent) and delayed settlement: Figure 3.

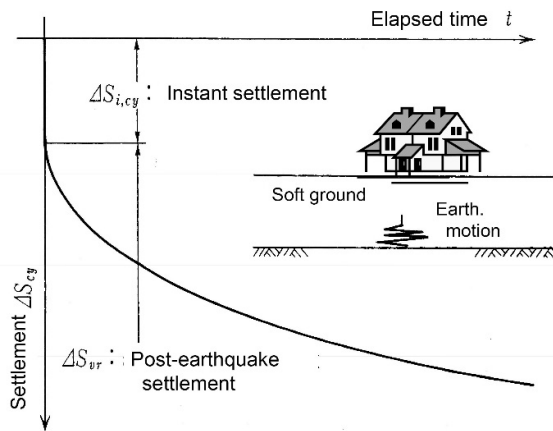


Figure 3 Constitution of earthquake-induced settlement of structures on cohesive soils

#### 3.2 Geotechnical Characteristics of Cohesive Soil Deposits beneath River Dykes and Private Residences

As stated earlier, one case in Ibaraki after the gigantic earthquake of 2011 showed settlement of thick cohesive soil deposits beneath the river dyke and private residences, thereby damaging river dykes and many adjacent private residences. The horizontal profiles of the

river dyke and residential areas portrayed in Figure 2 show a thick clay layer with 18 m deposits on the sand layer with higher ground water level (GWL). The plastic chart for this clay is shown in Figure 4 in which all plots are located along the A-line. Therefore, it seems that this clay is not specific to this point.

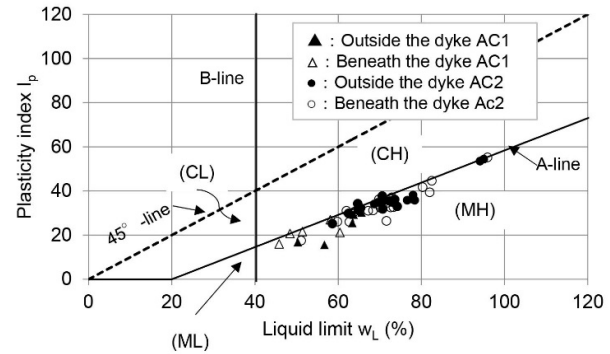


Figure 4 Plastic chart of K-clay in the objective site.

However, according to the summary of index and mechanical properties, this clay is also characterized by the following Yasuura & Kazama, 2015).

i) Highly sensitive with high liquidity index

ii) High water content with high undrained strength

Post-earthquake settlement is expected to result from consolidation followed by dissipation of excess pore pressures generated by a strong earthquake. The average index properties of clay are presented in Table 1. It is extremely unusual because characteristic (ii) does not make sense from geotechnical perspective, although characteristic (i) does make sense. This clay has high structures of clay particles, which readily undergo deformation by disturbance, leading to vertical settlement and lateral deformation. For comparison with K-clay clay in the objective site in the current study, Table 1 also shows index properties of J-clay for comparison, being deposited near the area of Joban express highway, which was constructed almost 35 years ago. Both clays are similar: both are highly plastic and become much softer with water contents beyond the liquid limit, although it cannot be said that the water content of either clay is very high.

Table 1 Index properties of clay beneath dykes in Ibaraki

Index	unit	K-clay	J-clay
Void ratio $e$		2.17	2.40
Density of soil particle $\rho_s$	$g/cm^3$	2.67	2.68
Wet density $\rho_t$	$g/cm^3$	1.52	-
Natural water content $w_i$	%	81.0	93.7
Liquid limit $w_L$	%	73.0	70.7
Plasticity limit $w_p$	%	37.0	28.8
Plasticity index $I_p$		36.0	41.9
Liquidity index $I_L$		1.20	1.20
Sensitivity ratio $S_t$		17.0	15.0
Unconfined compression strength $q_u$	$kN/m^2$	90.9	70.5

#### 3.3 Outlines of Settlement of River Dykes and Residences

A set of typical observed settlement vs. time relations for river dykes and residences continuously before and after the earthquake is presented in Figures 5 and 6. It is noteworthy that settlement took place and influenced the adjacent residences probably because of a

lack of installation of countermeasures having been undertaken along the river dykes. The figures also show that the earthquake occurrence in 2011 accelerated the settlement of river dykes and residences.

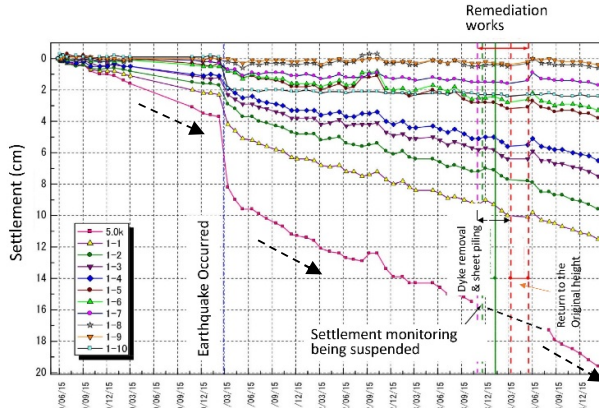


Figure 5 Settlement vs. time curves for river dykes

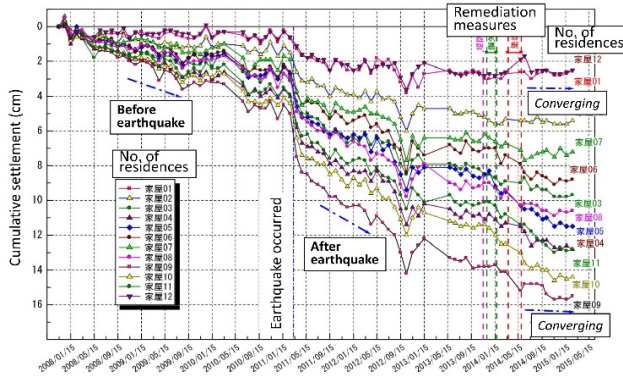


Figure 6 Settlement vs. time curves for residences.

As mentioned previously, settlement of cohesive soil deposits after the earthquake in 2011 was very complex, but it might be caused by combining the following.

- land sinking by crustal movement
- immediate settlement followed by deformation of upper sand and lower clay deposits, which is not time-dependent
- time-dependent settlement of clay deposits followed by dissipation of excess pore pressure generated by earthquakes.

This paper addresses issues (ii) and (iii) because it emphasizes an examination of post-earthquake behavior of clay deposits. The rates of settlement before and after the earthquake are noticeably different. The settlement has been exacerbated by earthquakes because of the post-earthquake settlement of clay deposits caused by delayed dissipation of excess pore pressure in clay deposits after the earthquake. Generally speaking, such settlement takes a long time to cease. Therefore, engineers and researchers must ascertain when the rate of residual settlement after the earthquake becomes negligible for residents not to feel at risk in everyday life.

Since 2007, the governmental office in charge of river management in the objective area has been monitoring variations of settlement, lateral displacement and excess pore water pressure (EPWP) over time inside and outside the river dykes. Results of settlement monitoring indicate the following.

- Settlement of residences accumulated up to 14 cm for the prior six years starting in 2007.

- Settlement increased to around 2 cm immediately after the earthquake in 2011.

### 3.4 Lateral Displacement Observation

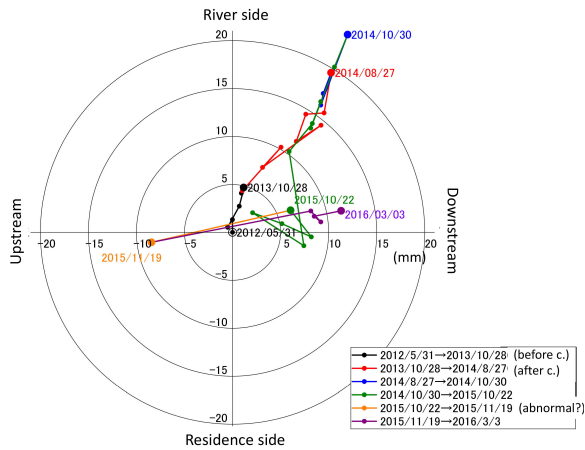
Borehole inclinometer installation at river dyke toes and borehole inclinometer measurements were conducted respectively from April 2009 to August 2011 and from May 2012 to March 2016. The monitored results presented in Figure 7 indicated the following.

- Inclination at the toes of dykes increased in the direction of residences before the earthquake. It tends to return to the dyke after the influence of the earthquake.
- Inclination tends to increase again towards the residences after the countermeasure execution but its magnitude is not so severe to influence on the residences.

Judging from the tendencies presented above, information of inclination monitored at the toe of dykes proves the effectiveness of the countermeasures adopted to avoid earthquake influences.



(a) April 2009 – August 2011



(b) May 2012 – March 2013

Figure 7 Measurement results of lateral displacement.

### 3.5 Results of Monitoring Excess Pore Water Pressure

Two sets of three piezometers for PWP measurement were installed in the clay layer beneath dykes and residences, as shown in Figure 8.

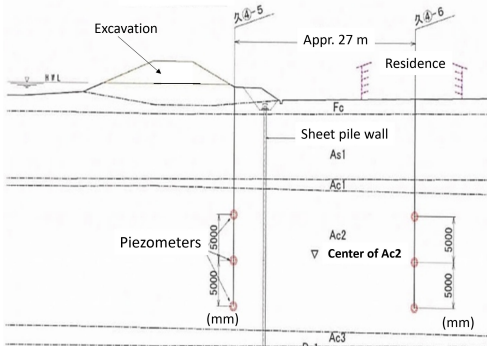


Figure 8 Installation of piezometers in the clay layer

Figure 9 presents an example of a set of the results of EPWP distribution and its variation with time from July 25 through August 8, 2013 at locations beneath the dyke and the residence.

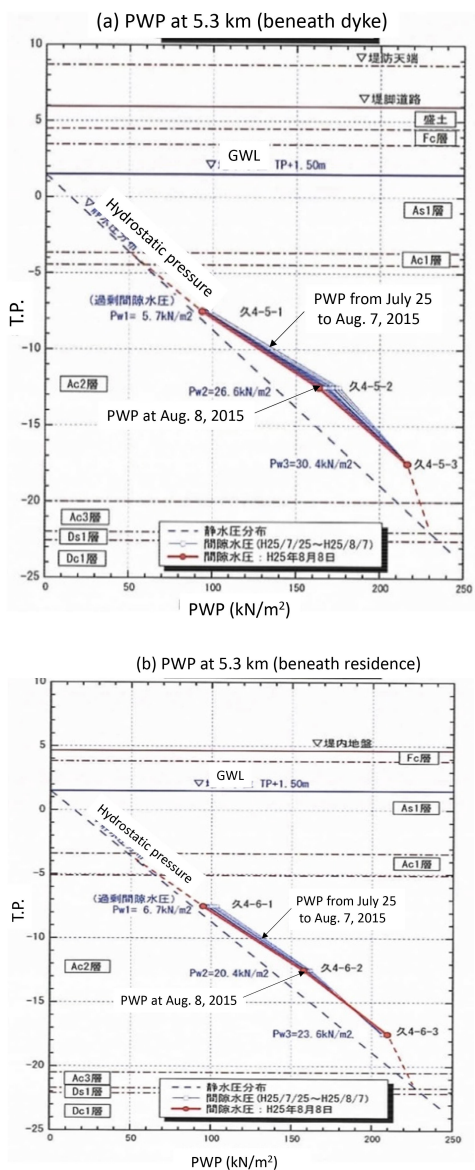


Figure 9 Variations of EPWP distribution with time at the location beneath the dyke and residence

Figure 9 shows that the EPWP at both sites remains after the earthquake but that the one beneath the residence is smaller than the other beneath the dyke although both remaining EPWPs tend to dissipate gradually throughout the clay layer, producing residual settlement at both sites.

Actually, however, EPWP behavior, particularly after the earthquake and installation of the countermeasures which will be described in the next chapter, is complicated. As shown in Figure 10, it is extremely difficult to predict the behavioral tendency precisely.

In spite of the present situation, the remaining EPWP,  $3.5 \text{ kN/m}^2$ , beneath the residence is less than that beneath the river dyke. This result must give some sense of security to residents.

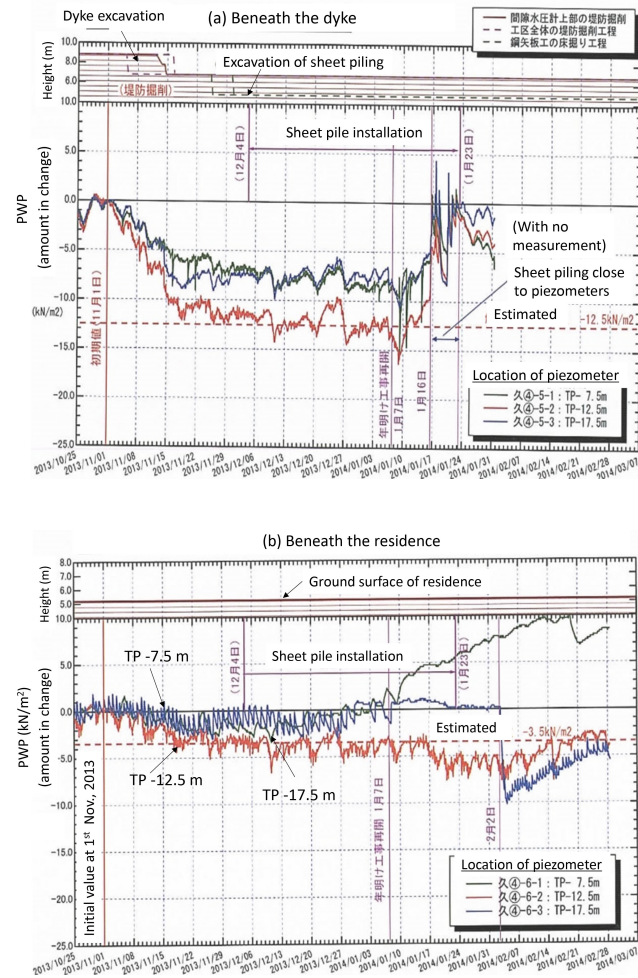


Figure 10 Variations of EPWP after the countermeasures

The following countermeasures were used to prevent effects of river dykes on post-earthquake settlement of residences (Figure 11).

- i) Remove 2.2 m of dykes to reduce dyke self-weight.
- ii) Thereafter, install sheet piles aside from the river dykes into the hard stratus, called  $A_{c3}$  layers, to intercept the effects of river dyke self-weight on residences.
- iii) Return the dyke height to the original height with 4.1 m.

As might be readily apparent from the results depicted in Figure 5 and Figure 6, the following behavior was observed after installing the countermeasures stated above.

- i) Remaining EPWP in subsoils both outside and inside the dykes became less than that before partial dyke removal.

As might be readily apparent from the results depicted in Figure 5 and Figure 6, the following behavior was observed after installing the countermeasures stated above.

- i) Remaining EPWP in subsoils both outside and inside the dykes became less than that before partial dyke removal.

- ii) Installation of sheet piles is associated with increased ground settlement beneath the dykes, but does not increase settlement of the ground outside the dykes. In other words, ground settlement beneath the residences might decrease.
- iii) Filling dykes again to their original height did not increase ground settlement of residences because of the intercept of stress distribution of dykes to residential ground.

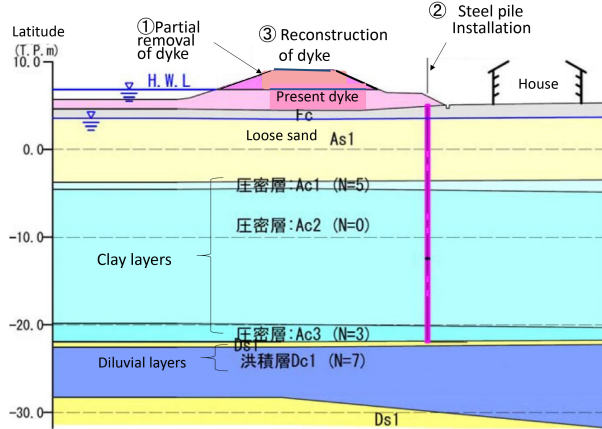


Figure 11 Remedial measures from damage induced by earthquake

As a summary of the tendencies described above, the countermeasures adopted herein have been effective for reducing post-earthquake settlement of residences near the river dykes. Furthermore, as described later, lateral displacement does not tend to increase towards the residences. However, continuous settlement monitoring should be done because groundwater abstraction effects on continuous settlement of residential areas remain uncertain.

## 5. NUMERICAL ANALYSIS

### 5.1 Analytical Procedures

To reproduce the behavior of dykes and their adjacent residences continuously from before to after the earthquake, numerical analysis using two-dimensional FEM was performed. The analytical flow is shown in Figure 12.

As the first stage for analysis, the excess pore pressures and their distribution in the subsoils under the self-weight of dykes were determined from the two-dimensional FEM analysis using computer code called Analysis for Liquefaction-induced Deformation (ALID). Using the seismic wave motion being measured under 500 m depth from the surface at a location 15 km distant from the river dyke with 6-week seismic intensity during the Tohoku Off-Pacific Earthquake in 2011, as shown previously in Figure 1, one-dimensional seismic response analysis was conducted.

The surface wave obtained from this analysis was input into ALID as the seismic motion. For these analyses, a Cam-clay model was adopted for predicting the excess pore pressures in Ac2 generated during the earthquake.

As the second stage, the elasto-viscoplastic two-dimensional FEM analysis using the computer code called Deformation Analysis Considering Stress Anisotropy and Reorientation (DACSAR) incorporating the Sekiguchi-Ohta model (Sekiguchi and Ohta, 1977; Iizuka & Ohta, 1987) was conducted to estimate settlement of river dykes and residences caused by dissipation of EPWP calculated using DACSAR.

### 5.2 Additional Parameters Necessary for Numerical Analysis

Additional parameters necessary for performing numerical analysis using DACSAR are summarized below.

- Coefficient of consolidation  $c_v$ : 0.046 ( $\text{m}^2/\text{day}$ )

- Coefficient volume compressibility  $m_v$ :  $1.38 \times 10^{-3}$  ( $\text{m}^2/\text{kN}$ ) calculated using the relation,  $m_v = 3\lambda / \{(1+e_0)(1+2K_0) \times \sigma' v_0\}$
- Coefficient of hydraulic conductivity  $k$  ( $\text{m}/\text{day}$ ) ( $k = m_v \cdot c_v \cdot \gamma_w$ ): 6.20  $\times 10^{-4}$
- Coefficient of secondary compression,  $\alpha$ :  $7.45 \times 10^{-3}$
- Initial volumetric strain rate,  $v_0$  ( $v_0 = \alpha/t$ ):  $1.21 \times 10^{-6}$  ( $1/\text{day}$ )

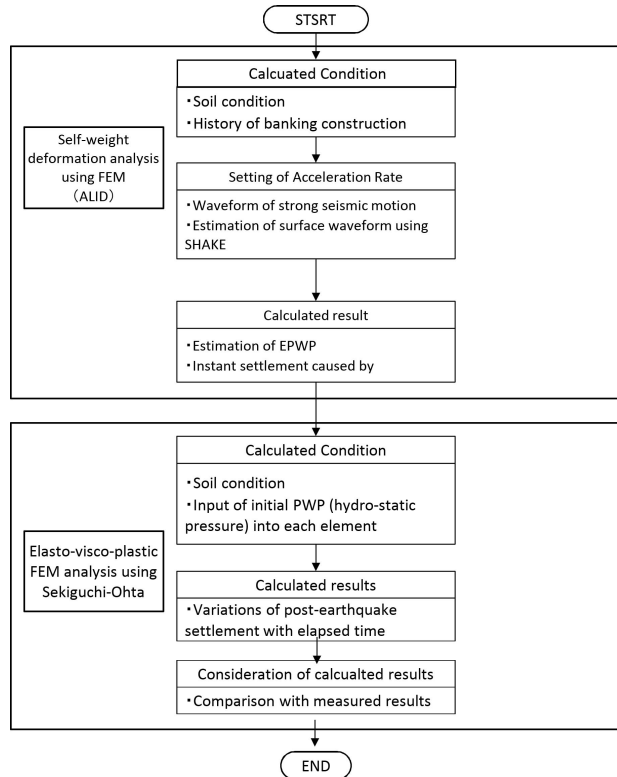


Figure 12 Flow chart of numerical analysis

### 5.3 Post-Earthquake Settlement and High Pore Water Pressure

As results of numerical analysis, calculated settlement and excess pore pressures are shown in Figure 13 and Figure 14. It can be indicated from both figures that

- i) Instant settlement of dykes was approximately 2 cm which is not large but lateral heaving was observed
- ii) EPWP was concentrated beneath the center of dykes

The EPWPs generated during the earthquake shown in Figure 13 were input as initial EPWP values into prediction of their variations in river dykes with elapsed time using DACSAR. The calculation results are shown in Figure 15 as distribution of EPWP against depth of river dykes. Particularly, results show that EPWP in thick clay layers generated during the earthquake tend to dissipate gradually and return to the original hydraulically static condition, but the maximum EPWP is generated directly beneath the river dyke.

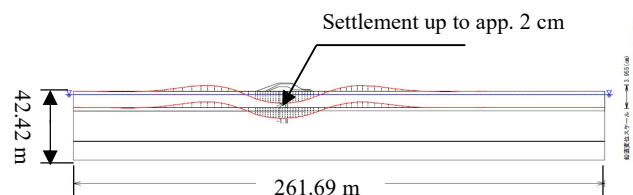


Figure 13 Settlement of dykes after earthquake

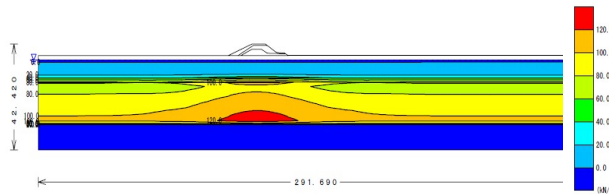


Figure 14 Distribution of EPWP generated by the earthquake

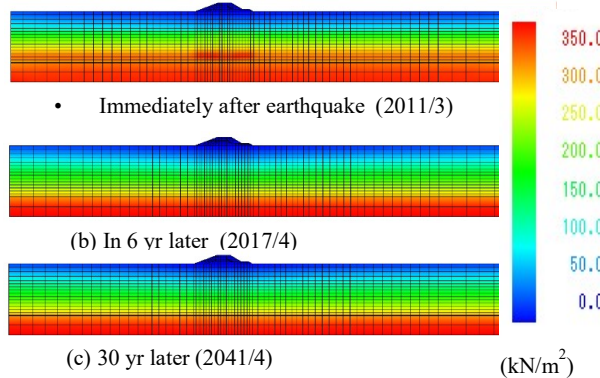


Figure 15 Variations of distribution of EPWP with elapsed time

Calculated settlement at the slope shoulder of the rear river is shown in Figure 16 for comparison with those measured. Figure 16 (a) demonstrates the following.

- The predicted total settlement of river dykes will be greater than 90 cm for the next 30 yr.
- Settlement must persist for more than 30 yr. In addition, Figure 15 (b) expanding the settlement vs. time relation during the 6 months after the earthquake indicates that the calculated settlement reaches 57.4 cm in 6 months after the earthquake, which is approximately four times the measured one as 14.8 cm.

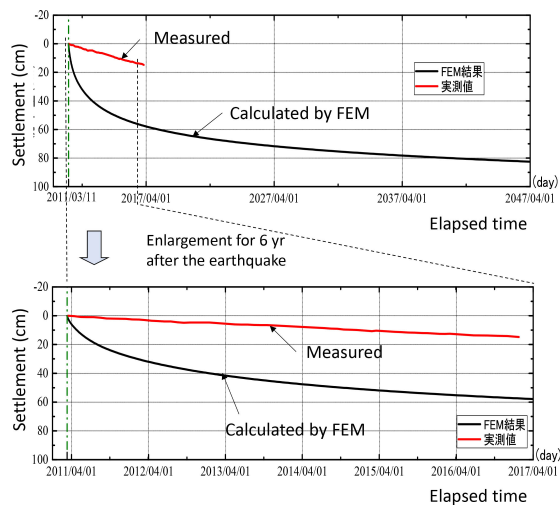


Figure 16 Calculated and measured settlement variations over time

Compression index,  $C_c$ , and secondary compression coefficient,  $C_\alpha$ , used for numerical analysis were obtained from odometer tests on undisturbed samples of  $A_{c2}$  layers. Those are demonstrated both in Figure 17 and Figure 18. It should be emphasized from those figures that the coefficient of secondary compression,  $C_\alpha$ , for  $A_{c2}$  in K-clay is 0.026 and the ratio,  $C_\alpha/C_c$ , is 0.024 in which both are normal in comparison with typical clays in Japan (i.e., Yasuhara and Ue, 1983).

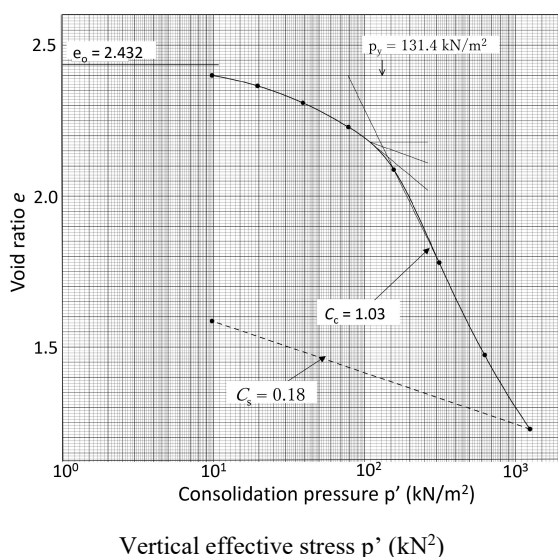


Figure 17 Void ratio vs. vertical stress relations on  $A_{c2}$

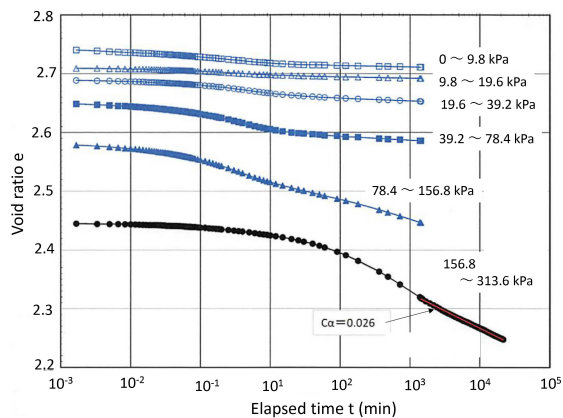


Figure 18 Void ratio vs. elapsed time relations on  $A_{c2}$  clays

According to comparison of calculated variations of settlement with elapsed time with the measured one as shown in Figure 16, there is no good agreement with both. Here, parameters related to long-term settlement of  $A_{c2}$  clay were re-determined using back analysis to adapt to the measured variations of settlement with time. The result calculated using the modified values of two parameters in the following way is shown in Figure 19.

In this case, good agreement exists between both calculated and simultaneously measured variations of settlement over time, indicating that long-term settlement of river dykes will continue, even for 30 yr.

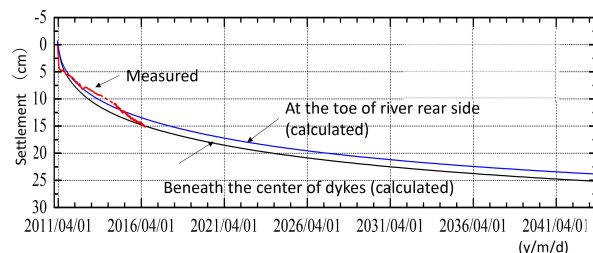


Figure 19 Recalculated and measured settlement variation over time

#### 5.4 Calculated Results of Lateral Displacement

Lateral displacement during and after an earthquake most strongly affects residents living near river dykes because earthquakes can show high lateral displacement, although the government started monitoring ten years ago in response to resident requests.

Figure 20 and Figure 21 present a family of calculated lateral displacement and inclination angle and settlement as a function of time elapsed from earthquake occurrence. Here, inclination angle  $\theta$  is defined as shown in Figure 22.

Figure 20 and Figure 21 presents the following.

- Lateral displacement tends to increase inland or at housing sites over time, which is similar to the measured tendencies in Figure 7.
- The magnitude of displacement is not large: less than 3 cm.

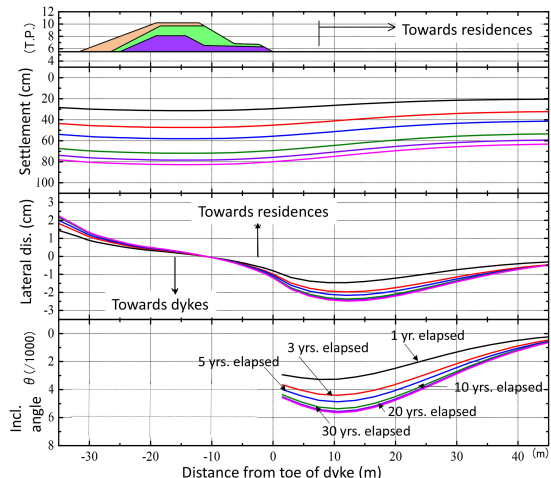


Figure 20 Calculated lateral displacement at the ground surface

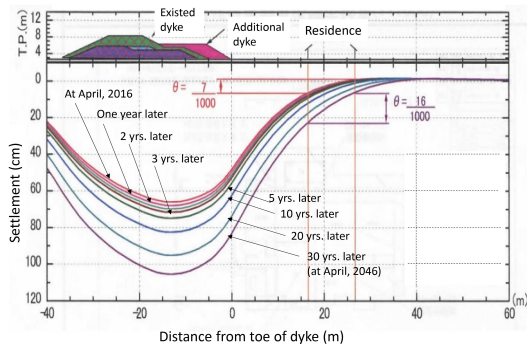


Figure 21 Variations of inclination angle with elapsed time

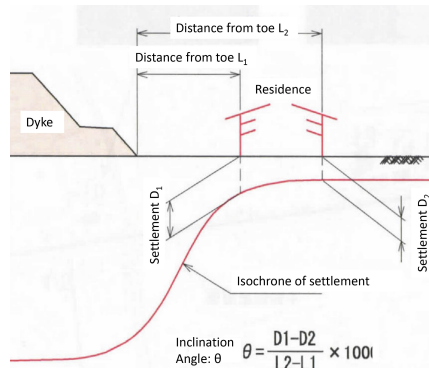


Figure 22 Inclination angle

#### 5.5 Evaluation of Countermeasure Effects

##### 5.5.1 Countermeasure Effects on Settlement

Effects of countermeasures as shown in Figure 18 were evaluated using the FE analysis. Figure 23 presents variations of settlement at the toes of banks at 30 yr after the earthquake. The parameters used for calculation were found using results of back calculation from measurements. Results are divided into two calculated curves with and without the countermeasures. Comparison between the curves shows their differences and clarifies effects of countermeasures on reducing dyke settlement, particularly after the earthquake.

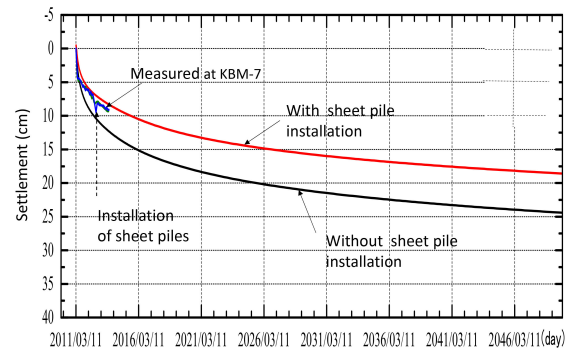


Figure 23 Calculated and measured settlement

##### 5.5.2 Countermeasure Effects on Lateral Displacement

In the same manner as that in the settlement computation, the calculated variations of lateral displacement over time with and without countermeasures are presented in Figure 24, divided into two cases at the toe of the river rear and the center of residences. The effects of countermeasures on reduction are also clear in these curves.

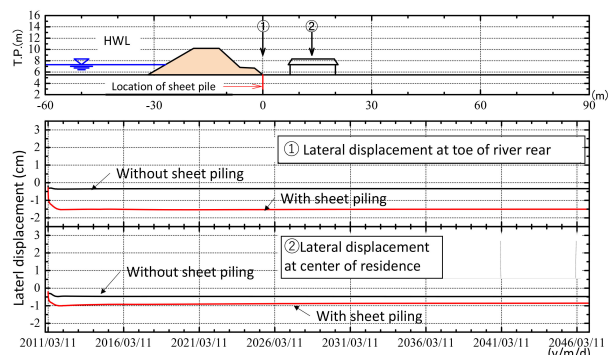


Figure 24 Calculated results of lateral displacement at dykes and residences with and without sheet pile installation

The same trend was observed in Figure 25 which shows the distribution of lateral displacement towards the depth of clay layers with and without countermeasures, suggesting that the countermeasures undertaken after the earthquake work particularly well for reducing damage in residences adjacent to the river dykes.

##### 5.5.3 Countermeasure Effects on Excess Pore Water Pressure

Successive to the computation of settlement and lateral displacement, computation of the variations of EPWPs with elapsed time was also conducted for three depths of clay soil layers with and without countermeasures. Among them, Figure 26 presents two cases beneath the dyke and the residence. Regarding EPWP behavior of in two locations, the countermeasure effects differ. That is, the larger

EPWP remains beneath the residence even 30 yr after the earthquake, but the smaller EPWP remains beneath the center of dykes. This persistence suggests that we should devote attention to the residual settlement of residences caused by dissipation of the larger EPWP remaining beneath the residence, although this tendency is not consistent with the measured settlement, as shown in Figure 6, which tends to converge at the present situation in 2015.

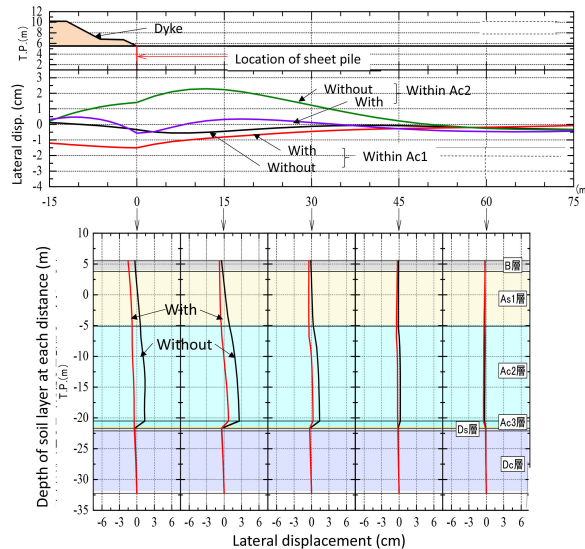


Figure 25 Lateral displacement against subsoil depth

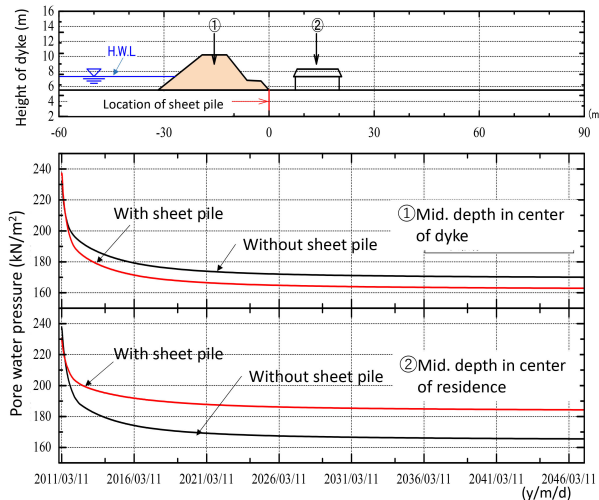


Figure 26 Calculated EPWP variations over time beneath dykes

## 6. CONCLUSION

The paper presents a description of our specific examination of post-earthquake settlement and deformation of clay layers beneath river dykes and their adjacent residences observed at some locations in the Kanto regions, as derived from a case history from this category of settlement in Ibaraki. After the earthquake in 2011, the MLIT adopted combined countermeasures by which a part of the dykes (1.5 m among 6.0 m in total) was removed initially. Then sheet piles were installed at the toes of dykes. Thereafter, the dykes were returned to the original height by surcharging. Investigations and numerical analyses of the case history suggest the following points.

- The combined countermeasures have worked effectively for reducing settlement and deformation not only in river dykes but also their adjacent residences founded on clay deposits.
- Numerical analysis using two computer programs suggests that countermeasures are beneficial for reducing dyke and residence settlement and lateral displacement on clay deposits.
- Careful attention must be devoted to the fact that such settlement and deformation are time-dependent. Therefore, monitoring of settlement and EPWP should continue for a long period.

## 7. ACKNOWLEDGEMENTS

Our great appreciation is extended to the Hitachi River and Road Office, Kanto branch, Ministry of Land, Infrastructure and Transport, which provided important information for this case study. The authors are also grateful for financial support from a Grant-in-Aid for Scientific Research from the Ministry of Education, Culture, Sports, Science and Technology (FY2016-FY2019, Project No. 16H02362), Japan, whose representative is Kazuya Yasuhara, Professor Emeritus of Ibaraki University, Japan.

## 8. REFERENCES

Iizuka, A. and Ohta, H. (1987). A determination procedure of input parameters in elasto-viscoplastic finite element analysis, *Soils and Foundations*, Vol. 27, No. 3, 71-87.

Imakiire, T. and Koarai, M. (2012). Wide-area land subsidence caused by the 2011 Off the Pacific Coast of Tohoku Earthquake, *Soils and Foundations*, Vol. 52, No. 5, 842-855.

Kazama, M. (2014). Geotechnical subjects seen to the damage of the 2011 off the Pacific Coast of Tohoku Earthquake, *Proc. 11<sup>th</sup> Symp. on Ground Improvement, Journal of Material Science, Japan*, pp. 1-20, (in Japanese).

Matsuda, H. (1996). Estimation of post-earthquake settlement-time relations of clay layer, *J. JSCE*, No. 568/III-39, 41-48 (in Japanese).

Matsuda, H., Nhan, T.T., Nakahara, D., Thien, D.Q. and Tuyen, T. H. (2014). Post-cyclic recompression characteristics of a clay subjected to undrained unidirectional and multi-directional cyclic shears, *Proc. Tenth U. S. National Conf. on Earthquake Engineering, Anchorage, AK*.

Sekiguchi, H. and Ohta, H. (1977). Induced anisotropy and time dependency in clays, *Proc. Ninth ICSMFE, Specialty Session 9*, Tokyo, pp.229-238.

Yasuda, S., Yoshida, N., Adachi, K., Kiku, H., Gose, S. and Masuda, T. (1999). A simplified evaluation method for evaluating lateral flow and subsequent liquefaction, *J. JSCE*, 638/III-49, 71-89 (in Japanese).

Yasuhara, K. and Ue, S. (1883). Increase in undrained strength due to secondary compression, *Soils and Foundations*, Vol. 23, No. 4, 50-64.

Yasuhara, K. and Andersen, K. H. (1991). Recompression of normally consolidated clay after cyclic loading, *Soils and Foundations, J. of JGS*, Vol. 31, No. 1, 83-94.

Yasuhara, K. and Matsuda, H. (1996). 5. Dynamic properties of cohesive soils (Part 2), Series: "Dynamic properties of cohesive soils", *J. of JGS*, Vol. 46, No. 12, 59-64 (in Japanese).

Yasuhara, K., Murakami, S., Toyota, N. and Hyde, A. F. L. (2001). Settlement in fine-grained soils under cyclic loading, *Soils and Foundations, J. of JGS*, Vol. 41, No. 6, 25-36.

Yasuhara, K. and Kazama, M. (2015). Land subsidence of clay deposits after the Tohoku-Pacific Ocean Earthquake (Keynote Lecture), *Proc. IAHS*, 372, 211-216, doi:10.5194/piahs-372-211-2015.